Comparison of Nonlinear Approximations to Gravitational Instability

By

B.S. Sathyaprakash, V. Sahni, D. Munshi, D. Pogosyan and A.L. Melott

Inter-University Centre for Astronomy & Astrophysics

An Autonomous Institution of the University Grants Commission

Comparison of nonlinear approximations to gravitational instability *

B.S. Sathyaprakash[1], V. Sahni[1], D. Munshi[1], D. Pogosyan[2], A. L. Melott[3]

[1]IUCAA Post Bag 4, Ganeshkhind, Pune 411 007, India
[2]CITA, University of Toronto, Ontario, Canada
[3]Department of Physics and Astronomy, University of Kansas, U.S.A.

Abstract. We compare different approximations to gravitational instability against N-body simulations in the strongly non-linear regime using a number of statistical indicators. We find that approximations such as frozen flow and linear potential breakdown soon after the non-linear length scale exceeds R_* – the mean distance between peaks of the gravitational potential – whereas others including the adhesion approximation, and to some extent, the truncated Zeldovich approximation, remain valid for later epochs, until the scale of nonlinearity approaches R_φ – the correlation length of the gravitational potential.

A simple means to test the accuracy of a given approximation to gravitational instability in relation to N-body simulations is provided by a statistical indicator such as the density-density correlation coefficient [1]. However, such tests are not sufficient to ascertain the usefulness of approximation schemes in understanding the formation and development of structural units such as clumps, filaments and voids. It is therefore helpful to employ statistical tools that are complementary and sometimes orthogonal to statistical indicators like the correlation coefficient, to discriminate between different approximation schemes [2,3]. In this two-dimensional study we compare (i) the Zeldovich approximation (truncated version – TZ), (ii) the adhesion model (AM), (iii) the frozen flow approximation (FF) and (iv) the linear potential approximation (LP) with the results of N-body simulations. After a visual inspection of the pictures produced by the different approximations we consider the following statistical discriminators for our comparatative study: (i) correlation coefficients. (ii) statistics of clumps, (iii) statistic quantifying filamentary behaviour, (iv) statistics of voids and (v) the void probability function, each of which single out certain features of non-linear clustering. The domain of validity of a given approximation is therefore discussed with reference to a given statistical indicator.

Two natural scales characterizing the primordial gravitational potential are suitable for providing bounds on the validity of the different approximations. These are: (i) the scale R_*, corresponding to the average distance between the peaks of the potential and (ii) the scale R_φ characterizing the correlation length of the potential ($R_\varphi \geq R_*$). R_φ and R_* can be expressed in terms of the spectrum $P(k)$ and the moments of the potential field σ_j by

$$R_\varphi = \sqrt{2}\frac{\sigma_0}{\sigma_1}, \quad R_* = \sqrt{2}\frac{\sigma_1}{\sigma_2}, \quad \text{where} \quad \sigma_j^2 \propto \int_{k_f}^{k_c} k^{2j-4} P(k) k \, dk, \tag{1}$$

where k_f is the fundamental mode and k_c is an upper cutoff in the spectrum of fluctuations [3,4].

$\sigma=32$ $\sigma=128$

NB   NB

AA   AA

LP   LP

$\sigma=32$ $\sigma=128$

FF FF

TZ TZ
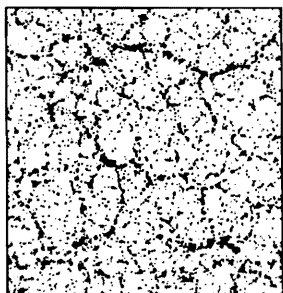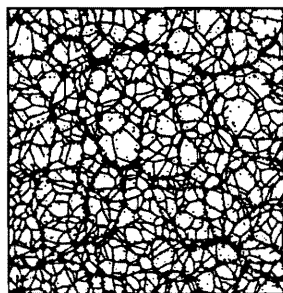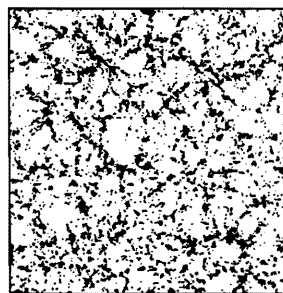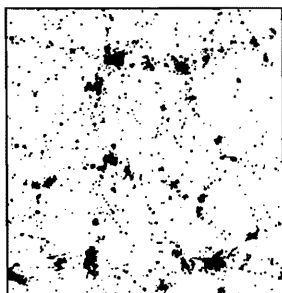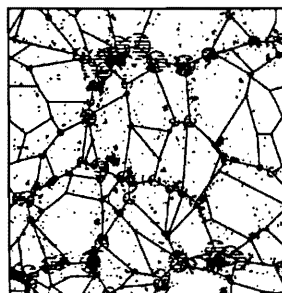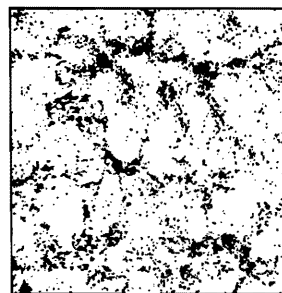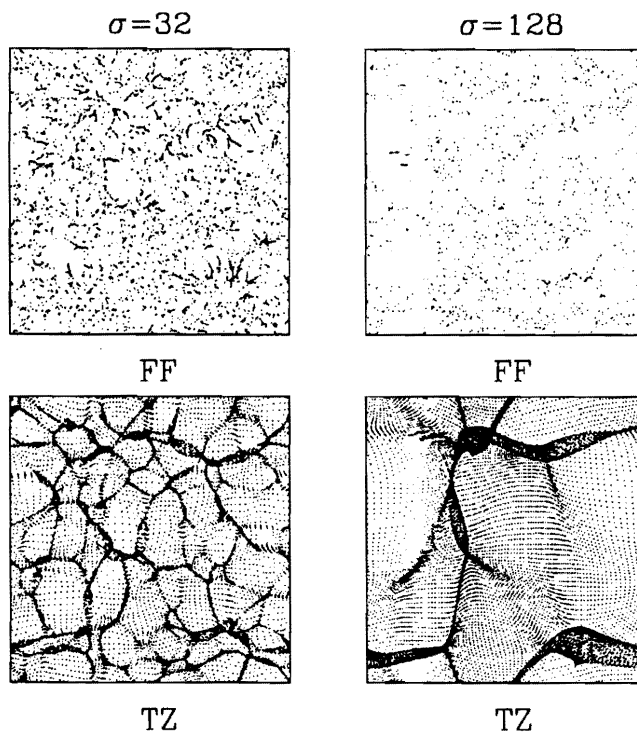
Fig. 1. Comparison of N-body simulations with the simulations of various approximation schemes. This and the rest of the figures correspond to the power-law model $P(k) \propto k^n$ for $k < k_c$ and $P(k) = 0$ otherwise with $n = 0$ and $k_c = 256k_f$. Simulations are performed in 2-d using 512×512 particles. From top to bottom the pictures correspond to N-body, adhesion model superposed on N-body, linear potential, frozen flow, and truncated Zeldovich approximation, respectively. The left and the right panels are obtained at epochs $\sigma \sim \sigma_*$ and $\sigma \sim \sigma_\varphi$, respectively.

The structure obtained using the AM and the evolved particle positions in the case of FF, LP and TZ are shown in Fig. 1. In terms of the *rms* density contrast on the grid scale $-\sigma$, the left hand panels correspond to an epoch $\sigma \sim \sigma_*$ ($k_{NL}^{-1} \sim R_*$) and the right panels to an epoch $\sigma \sim \sigma_\varphi$ ($k_{NL}^{-1} \sim R_\varphi$).

We find that for epochs $\sigma \leq \sigma_*$, leading up to the completion of cellular structure, all approximation schemes reproduce the structure with roughly the same accuracy as in N-body simulations. Later epochs are characterised by the motion and mergers of filaments and clumps due to their mutual attraction as well as their repulsion by underdense regions – two dimensional voids.

From the right panels it is clear that close to the epoch when the scale going nonlinear is R_φ the structure obtained using AM is still in excellent visual agreement with that of N-body simulations. TZ has a reasonably good visual agreement with N-body on large scales though at this epoch the small scale features abundant in N-body simulations are not reproduced in the TZ simulation. Particle dynamics in LP and FF is at all times determined by the gradients of the local primordial potential [5,6,7]. However we know from N-body simulations that the small scale features of the primordial potential play little, if any, role in the furtherance of gravitational clustering at late times. It therefore might be expected that LP and FF will not be able to reproduce even qualitatively the late-time features of hierarchical clustering. This is in fact confirmed by the right hand panels in Fig. 1. The visual agreement of AM and TZ with N-body lasts for epochs $\sigma \gg \sigma_*$ since these two approximations use power on successively larger scales to influence the dynamics of particles [1,8,9]. Thus as long as the initial potential has sufficient large scale power to give rise to coherent motion over large scales, TZ and AM are expected to remain approximately valid.

One is often interested in the evolution of the density field since it allows us to infer the evolution of many other structural units such as clumps, filaments and voids. The correlation coefficient of two density (contrast) fields δ_1 and δ_2 is defined by:

$$r_\delta \equiv \frac{\sum_i \delta_1^i \delta_2^i}{\left[\sum_j (\delta_1^j)^2 \sum_k (\delta_2^k)^2\right]^{1/2}}. \tag{2}$$

The evolution of the statistic r_δ is shown in Fig. 2. We notice that TZ and AM are in better agreement with N-body than FF and LP. (This should be contrasted with Fig. 1 wherein the visual agreement of TZ with N-body is not so remarkable. The density correlation on the other hand indicates good agreement up to very late times.) The reason why FF and LP fare badly at late times $\sigma > \sigma_*$ can be traced to Fig. 1 wherein we see that by the epoch σ_* matter has completely emptied out into rivulets determined by wells of the potential in the case of FF. In LP matter tends to oscillate about the potential minima. Thus, large scale structure does not show much quantitative evolution beyond the epoch $k_{NL}^{-1} \simeq R_*$ in both approximations.

In Fig. 3 we have shown the evolution of the number of clumps. Following the N-body curve (thick solid line) we see that there are two distinct phases in the clustering of matter via gravitational instability. During the first phase the number of clumps keeps increasing reaching a maximum when $\sigma \sim \sigma_*$, at which time the formation of cellular structure is complete. During the second phase ($\sigma > \sigma_*$) clustering proceeds hierarchically as smaller clumps merge to form clumps of larger mass. $\sigma \simeq \sigma_*$ characterizes the epoch of the transition from the cellular to the hierarchical phase of clustering [10].

We note that with the exception of AM none of the other approximations reproduce the expected fall-off in the number of clumps at late times caused by clump merger. In FF
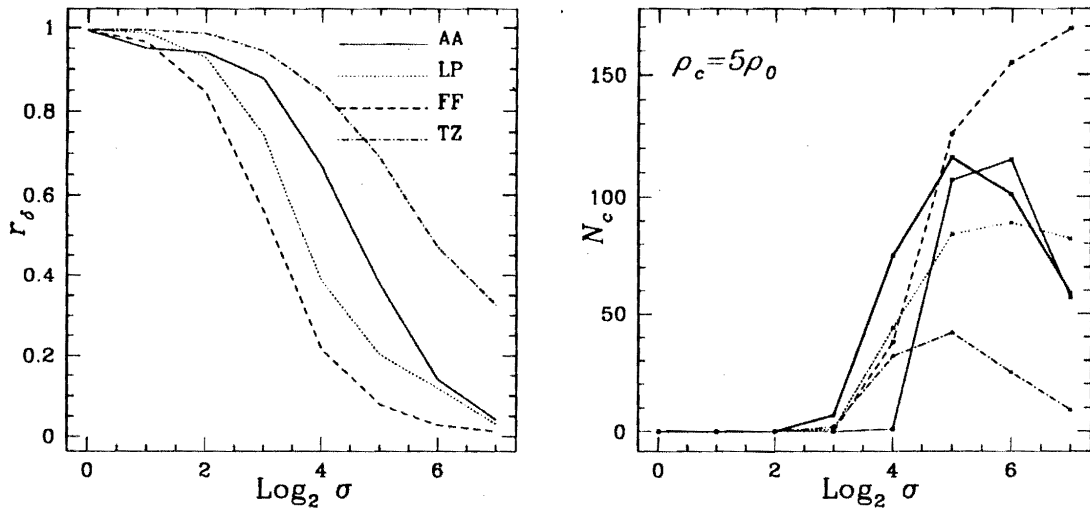
Fig. 2. (Left) Evolution of the density correlation coefficient corresponding to (i) adhesion model (solid line), (ii) frozen flow (dashed line), (iii) linear potential (dotted line), and (iv) Zeldovich (dashed-dotted line).

Fig. 3. (Right) Evolution of the number of clumps. Curves are as in Fig. 2 except that here we have the results corresponding to N-body in thick solid line.

and LP the number of clumps, at earlier epochs, show the general trend of a sharp rise and closely resemble the predictions of N-body simulations till about σ_*. However, in neither FF nor LP does the clump number decrease after this epoch, indicating that mergers are not properly described in these approximations. We note that the statistics of clumps produced by TZ is almost never in agreement with N-body simulations. The reason for this is that in this approximation the clumps are at no time well defined objects.

We define individual voids as connected regions of a given underdensity. The evolution of the number of voids plotted in Fig. 4 exhibits behaviour similar to the evolution of clumps seen in Fig. 3. With reference to the N-body curve (thick solid line) we observe that the number of voids first rises sharply, approaches a maximum value at $\sigma \simeq \sigma_*$ and thereafter falls steadily, more or less stabilizing after a while. Voids are not well defined objects at very early epochs ($\sigma \leq 1$) but by the epoch σ_* they gain their identity. The decline in the number of voids in Fig. 4 is a consequence of the fact that voids compete for space as the Universe expands, and that smaller voids can be encroached upon by larger ones. Thus, voids not only expand they can also contract and ultimately disappear during the hierarchical epoch of clustering [10].

From Fig. 4 we find that the adhesion model produces roughly the right evolution for the number of voids whereas FF and LP fail to do so. In the case of FF as matter falls into deeper wells of the potential, the cellular structure gets completely phased out with the result that at later epochs very few voids are left behind in this case. In other words, in FF there is no cellular structure to "support" the voids. The same is true in the case of LP but because of the fact that the particles do cross over caustic regions the cellular structure lasts a little longer and the fall off in the number of voids is somewhat slower than in the case of FF. TZ, as expected from Fig. 1, always predicts fewer but larger voids as compared to N-body. To conclude we find that at early epochs all approximations give similar results but at later times AM and TZ perform better than FF and LP. (For results obtained using other statistical indicators see Sathyaprakash et al. [3]).
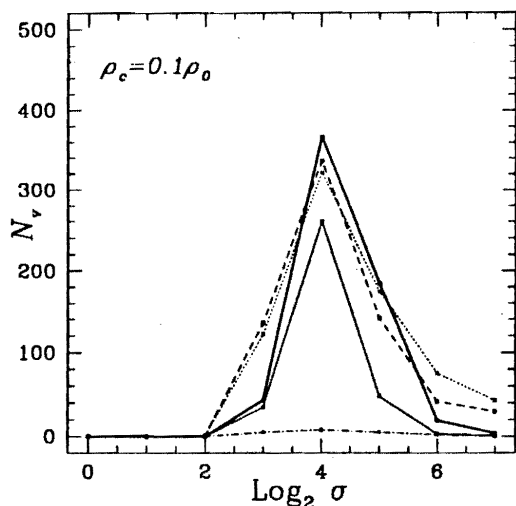
Fig. 4. Evolution of the number of voids. Curves are as in Fig. 3.

References

[1] Coles, P, Melott, A.L., & Shandarin, S.F., 1993, MNRAS, 260, 765

[2] Sahni, V. & Coles, P., 1995, Phys. Rep. in press

[3] Sathyaprakash, B.S., Sahni, V., Munshi, D., Pogosyan, D. & Melott, A.L., 1995, MNRAS (submitted)

[4] Kofman, L. A., Pogosyan, D. Yu., Shandarin, S. F., & Melott, A. L., 1992, ApJ, 393, 437

[5] Matarrese, S., Lucchin, F., Moscardini, L., & Saez, D., 1992, MNRAS, 259, 437

[6] Brainerd, T.G., Scherrer, R.J., & Villumsen, J.V., 1993. ApJ, 418, 570

[7] Bagla, J.S., & Padmanabhan, T., 1994. MNRAS, 266, 227

[8] Gurbatov, S. N., Saichev, A. I., & Shandarin, S. F., 1985, Soviet Phys. Dokl. 30, 921

[9] Zeldovich, Ya.B., 1970, A&A, 4, 84

[10] Sahni, V., Sathyaprakash, B.S., & Shandarin, S.F., 1994, ApJ, 431, 20